AIAA JOURNAL
Vol. 43, No. 12, December 2005

Modeling of Aeroservoelastic Systems with Structural and Aerodynamic Variations

Boris Moulin*
Technion—Israel Institute of Technology, 32000 Haifa, Israel

A procedure for modeling of aeroservoelastic systems with structural and aerodynamic variations and uncertainties is presented. The structural variations are associated with deviations in stiffness, mass, and damping structural parameters, whereas the aerodynamic variations are defined by the deviations in aerodynamic influence coefficients. A model of the perturbed system is constructed in the form of a linear fractional transformation relating the nominal system dynamics with the variations of its structural and aerodynamic properties. The developed technique enables modeling of perturbed aeroservoelastic systems in both frequency and time domains. The models are compatible with standard robust analysis and control design procedures such as μ technique used in the numerical example. The structural and aerodynamic variations are expressed in discrete coordinates that can also be transformed into modal coordinates. The discrete-coordinate representation enables size reduction of the uncertainty matrices for local structural and aerodynamic variations with respect to the modal representation. This is important for robust analysis and control design. A numerical application for an uncrewed aerial vehicle is used to demonstrate the modeling process. Models of the open- and closed-loop aeroservoelastic systems augmented with inertial and aerodynamic uncertainties of the control surface are constructed and applied for robust stability analysis.

Nomenclature

$[A_{h0,1,2}]$, $[D_h]$, $[E]$	=	rational approximation matrices for the nominal generalized aerodynamic forces
$[A_{r_a v_a 0,1,2}]$, $[D_{r_a}]$, $[E_{v_a}]$	=	rational approximation matrices for the aerodynamic variation
$[A_{(.)}]$, $[B_{(.)}]$, $[C_{(.)}]$, $[D_{(.)}]$	=	state-space matrices
$[\mathrm{AIC}_{r_a v_a}]$	=	matrix of the aerodynamic variation
b	=	reference semichord
$\mathcal{F}_u$, $\mathcal{F}_\ell$	=	upper and lower linear fractional transformation (LFT)
$[G]$	=	spline matrix
$[G_V]$	=	controller gain matrix
$[I]$	=	identity matrix
$[M_{hc}]$	=	mass coupling matrix between control and structural modes
$[M_{hh}]$, $[B_{hh}]$, $[K_{hh}]$	=	generalized mass, viscous damping, and stiffness matrices of the nominal system
$[M_{vv}]$, $[B_{vv}]$, $[K_{vv}]$	=	mass, viscous damping, and stiffness matrices of the structural variation
n_c, n_G, n_h	=	number of control surfaces, gust excitations, and normal modes
n_v, n_{r_a}, n_{v_a}	=	size of the v, the r_a, and the v_a sets
$\bar{P}$	=	transfer matrix of the augmented aeroelastic system
$[Q_{hh}]$, $[Q_{hc}]$, $[Q_{hG}]$	=	nominal aerodynamic matrices associated with generalized displacements, control surface commanded deflections, and gust velocity vector
q	=	dynamic pressure
$[R]$, $[R_\Delta]$	=	aerodynamic lag matrices for the nominal aerodynamic forces and the aerodynamic variation
s	=	Laplace transform variable
V	=	true airspeed
W_l, W_r	=	left and right weighting matrices
W_s	=	scailing matrix
w_G	=	gust velocity vector
$\{x\}$, $\{u\}$, $\{y\}$	=	state, input and output vectors
$\{x_a\}$	=	aerodynamic augmented states
$\bar{\Delta}$, Δ	=	absolute and normalized variations
$\bar{\Delta}_{\mathrm{st}}$, $\bar{\Delta}_a$	=	matrices of structural and aerodynamic variations
$\bar{\Delta}_0$	=	fixed part of the absolute variation
$\{\delta_c\}$	=	control-surface commanded deflections
$\{\xi\}$	=	generalized displacements
$\{\phi_{gh}\}$	=	normal modes in the structural set
$\{\phi_{kh}\}$	=	normal modes in the aerodynamic set
$\{\phi_{vh}\}$, $\{\phi_{v_a h}\}$, $\{\phi_{r_a h}\}$	=	normal modes in the v-, the v_a-, and the r_a-sets
$\{\phi_{yh}\}$	=	normal modes for the output degrees of freedom
ω	=	frequency

Subscripts and Superscripts

a	=	aerodynamic variation
ac	=	actuators
ae	=	open-loop aeroelastics
ase	=	closed-loop aeroservoelastics
c	=	control modes or controller
G	=	gust excitation
h	=	structural modes
p	=	open-loop aeroelastics with actuators
r_a	=	set of aerodynamic degrees of freedom effected by the aerodynamic variation
st	=	structural variation
V	=	gain-open aeroservoelastic system
v, v_a	=	sets of degrees of freedom involved in the structural (v-set) and the aerodynamic (v_a-set) variations

Presented as Paper 2004-1675 at the AIAA/ASME/ASCE/AHS/ASC 45th Structures, Structural Dynamics, and Materials Conference, Palm Springs, CA, 19–22 April 2004; received 9 December 2004; revision received 15 May 2005; accepted for publication 30 June 2005.

*Senior Researcher, Faculty of Aerospace Engineering. Member AIAA.

w = disturbance input
δ = augmented structural and aerodynamic variations

I. Introduction

MODERN methods of robust aeroelastic and aeroservoelastic (ASE) analysis and control design for aeroelastic systems require modeling of flight vehicles undergoing structural and aerodynamic variations or uncertainties. Models of perturbed ASE systems are formulated in the form of linear fractional transformation (LFT) in frequency or time domain. Lind and Brenner[1] showed how uncertainties can be modeled and used for calculation of robust stability margins. This modeling approach was extended in Ref. 2 and used for a match-point robust flutter analysis in a state space. Borglund[3,4] presented the frequency-domain aeroelastic models considering aerodynamic uncertainty in matrix coefficients of the Roger's rational approximation and in the frequency-domain pressure coefficients. The procedure for structural and robust control design of aeroservoelastic systems with structural variations and/or uncertainties was presented in Ref. 5. It was applied to a sample aircraft model with uncertainties in its tip-store inertial properties.

An essential part of robust ASE analysis and control design is modeling of uncertain open- and closed-loop aeroelastic systems. The current study presents a technique for modeling of ASE systems perturbed by structural and aerodynamic variations. This technique extends and generalizes the methodology developed in Ref. 5 and presents a unified procedure for modeling of ASE systems undergoing structural and aerodynamic variations. Uncertainty models are derived in discrete coordinates so that the variation matrices include structural and aerodynamic parameters (stiffness, mass, damping, and aerodynamic influence coefficients) for the discrete degrees of freedom of the perturbed part of the aeroelastic system. This leads to size reduction of the uncertainty matrices for local structural and aerodynamic variations compared with their modal representation. This is important, for instance, for effectiveness of structural singular value computation and for μ-control design because the dimension and, thus, complexity of a μ controller depends on the size of the uncertainty block. Constructed uncertainty models can be also transformed into modal coordinates. The developed technique enables modeling of perturbed ASE systems in both frequency and time domains. The modeling procedure allows consideration of gust excitation. This modeling technique is then applied to a sample uncrewed aerial vehicle (UAV) with uncertainties in inertial and aerodynamic properties of its control surface. The modeling procedure is followed by a robust stability analysis of the open-loop aeroelastic and closed-loop ASE systems. The numerical example is instrumental in demonstrating the effectiveness of the proposed modeling technique.

II. Second-Order Equations of Motion of Aeroelastic System with Structural and Aerodynamic Variations

The open-loop aeroelastic equations of motion of the nominal system excited by control-surface deflection commands and by gust can be expressed in Laplace domain as

$$\begin{aligned}&\left([M_{hh}]s^2+[B_{hh}]s+[K_{hh}]+q[Q_{hh}(s)]\right)\{\xi(s)\}\\&\quad=-\left([M_{hc}]s^2+q[Q_{hc}(s)]\right)\{\delta_c(s)\}\\&\quad-(q/V)[Q_{hG}(s)]\{w_G(s)\}\end{aligned}\tag{1}$$

where V is the air velocity and $[Q_{hh}(s)]$, $[Q_{hc}(s)]$, and $[Q_{hG}(s)]$ are the nominal aerodynamic matrices associated with generalized displacements $\{\xi(s)\}$, control surface commanded deflections $\{\delta_c(s)\}$, and gust velocity vector $\{w_G(s)\}$.

Structural variation is considered as deviations in mass, stiffness, and damping properties of the nominal structure that do not lead to changes in the number of structural degrees of freedom of the system. The structural variation is defined by its mass $[M_{vv}]$, stiffness $[K_{vv}]$, and damping $[B_{vv}]$ matrices associated with the v set of degrees of freedom involved in the variation. The v set includes all of the degrees of freedom associated with the mass, stiffness, and damping variations, so that the $[M_{vv}]$, $[K_{vv}]$, and $[B_{vv}]$ matrices may contain zero rows and columns. For example, the zero rows and columns of the matrix $[M_{vv}]$ correspond to the degrees of freedom associated with stiffness and/or damping perturbations exclusively.

Aerodynamic variation is defined as a deviation of the aerodynamic influence coefficients (AIC) of the nominal aerodynamic model. The AIC matrices can be calculated by unsteady aerodynamic codes for prescribed reduced-frequency $k=\mathrm{Im}(sb/V)$ values, where b is the reference semichord. In this study, the aerodynamic variations are considered for the AIC matrices calculated based on any panel method (e.g., Refs. 6 and 7). The variations to be considered do not lead to changes in the number of aerodynamic degrees of freedom of the baseline system. The $n_{r_a}\times n_{v_a}$ matrix $[\mathrm{AIC}_{r_a v_a}(s)]$ of the aerodynamic variation defines the perturbation of the aerodynamic forces applied to the r_a set of aerodynamic degrees of freedom caused by the unit deflections in the v_a set of degrees of freedom involved in the aerodynamic variation. The r_a set includes all of the aerodynamic degrees of freedom or its subset (when the effect of the v_a set deflections on the aerodynamic forces in some degrees of freedom can be considered as negligible). The aerodynamic variation $[\mathrm{AIC}_{r_a v_a}(s)]$ is the frequency-dependent complex rectangular matrix.

The fixed-basis modal approach adopted in the paper assumes that the structural displacements of the modified or perturbed system can be adequately expressed as a linear combination of the baseline normal modes $[\phi_{gh}]$ in the structural set. The displacements and slopes of the aerodynamic boxes are obtained from the structural displacements using the spline matrix $[G]$, so that the normal modes $[\phi_{kh}]$ in the aerodynamic degrees of freedom are expressed as $[\phi_{kh}]=[G][\phi_{gh}]$. Hence, applying the fixed-basis modal approach, the aerodynamic displacements of the modified system are expressed as a linear combination of the baseline normal modes $[\phi_{kh}]$.

The equation of motion of the modified structure perturbed by the variations of its mass, damping and stiffness parameters and by the variation of the elements of the AIC matrix can be written as

$$\begin{aligned}&\left([M_{hh}]_m s^2+[B_{hh}]_m s+[K_{hh}]_m+q[Q_{hh}(s)]_m\right)\{\xi(s)\}\\&\quad=-\left([M_{hc}]_m s^2+q[Q_{hc}(s)]_m\right)\{\delta_c(s)\}\\&\quad-(q/V)[Q_{hG}(s)]_m\{w_G(s)\}\end{aligned}\tag{2}$$

where the modal matrices of the modified structure are expressed as

$$[M_{hh}]_m=[M_{hh}]+[\phi_{vh}]^T[M_{vv}][\phi_{vh}]$$

$$[M_{hc}]_m=[M_{hc}]+[\phi_{vh}]^T[M_{vv}][\phi_{vc}]$$

$$[B_{hh}]_m=[B_{hh}]+[\phi_{vh}]^T[B_{vv}][\phi_{vh}]$$

$$[K_{hh}]_m=[K_{hh}]+[\phi_{vh}]^T[K_{vv}][\phi_{vh}]$$

$$[Q_{hh}(s)]_m=[Q_{hh}(s)]+\left[\phi_{r_a h}\right]^T\left[\mathrm{AIC}_{r_a v_a}(s)\right]\left[\phi_{v_a h}\right]$$

$$[Q_{hc}(s)]_m=[Q_{hc}(s)]+\left[\phi_{r_a h}\right]^T\left[\mathrm{AIC}_{r_a v_a}(s)\right]\left[\phi_{v_a c}\right]$$

$$[Q_{hG}(s)]_m=[Q_{hG}(s)]+\left[\phi_{r_a h}\right]^T\left[\mathrm{AIC}_{r_a v_a}(s)\right]\left[\phi_{v_a G}\right]$$

where $[\phi_{vh}]$ is the $n_v\times n_h$ matrix of the normal modes for the v set, $[\phi_{r_a h}]$ and $[\phi_{v_a h}]$ are the matrices of the normal modes for the r_a set and the v_a set aerodynamic degrees of freedom, $[\phi_{vc}]$ and $[\phi_{v_a c}]$ are the v and v_a partitions of the control modes in the structural and aerodynamic sets, $[\phi_{v_a G}]$ is the v_a partition of the gust mode in the aerodynamic set, n_v is the size of the v set, and n_h is the number of the normal modes.

Rewrite Eq. (2) as follows:

$$\begin{aligned}&\Big([M_{hh}]s^2+[B_{hh}]s+[K_{hh}]+q[Q_{hh}(s)]\Big)\{\xi(s)\}\\&\quad=-\Big([M_{hc}]s^2+q[Q_{hc}(s)]\Big)\{\delta_c(s)\}-(q/V)[Q_{hG}(s)]\{w_G(s)\}\\&\quad-[\phi_{vh}]^T\Big([M_{vv}]s^2+[B_{vv}]s+[K_{vv}]\Big)\{u_v(s)\}\\&\quad-q\Big[\phi_{r_ah}\Big]^T\Big[\mathrm{AIC}_{r_av_a}(s)\Big]\Big\{u_{v_a}(s)\Big\}-[\phi_{vh}]^T[M_{vv}][\phi_{vc}]s^2\{\delta_c(s)\}\\&\quad-q\Big[\phi_{r_ah}\Big]^T\Big[\mathrm{AIC}_{r_av_a}(s)\Big]\Big[\phi_{v_ac}\Big]\{\delta_c(s)\}\\&\quad-(q/V)\Big[\phi_{r_ah}\Big]^T\Big[\mathrm{AIC}_{r_av_a}(s)\Big]\Big[\phi_{v_aG}\Big]\{w_G(s)\}\end{aligned}\tag{3}$$

where the structural $\{u_v\}$ and the aerodynamic $\{u_{v_a}\}$ displacements for the degrees of freedom involved in the structural and aerodynamic variations are presented as

$$\{u_v(s)\}=[\phi_{vh}]\{\xi(s)\}\tag{4}$$

$$\Big\{u_{v_a}(s)\Big\}=\Big[\phi_{v_ah}\Big]\{\xi(s)\}\tag{5}$$

The first two terms on the right-hand side of Eq. (3) represent the nominal forces due to control-surface commanded deflections and gust. All of the next terms are induced by the variations: the third and the fifth terms represent the modal inertial, damping, and elastic forces and the inertial forces due to the mass coupling between the aircraft and the control surfaces inserted by the structural variation. The fourth, sixth, and the seventh terms represent the additional aerodynamic forces induced by the aerodynamic variation and associated with elastic deformations, control-surface commanded deflections, and gust.

Equations (3–5) are equivalent to Eq. (2), but the model of Eqs. (3–5) is cast in the form of a system with feedback representing the dynamics induced by the structural and aerodynamic variations.

Output displacements can be cast by the mode-displacement approach as

$$\{y_{\mathrm{ae}}(s)\}=[\phi_{yh}]\{\xi(s)\}\tag{6}$$

where $[\phi_{yh}]$ is the matrix of the normal modes for the output degrees of freedom.

III. Model of Perturbed Open-Loop Aeroelastic System

The model of the perturbed aeroelastic system represented by Eqs. (3–5) can be expressed as a system of linear first-order equations in the Laplace domain to facilitate the frequency-domain solution and incorporation of the control system state-space equations.

Define the matrices of the structural and aerodynamic variations and the corresponding vectors that multiply them from the right-hand side as

$$\bar{\Delta}_{\mathrm{st}}=\begin{bmatrix}[K_{vv}]&0&0\\0&[B_{vv}]&0\\0&0&[M_{vv}]\end{bmatrix},\qquad \bar{\Delta}_a(s)=\Big[\mathrm{AIC}_{r_av_a}(s)\Big]$$

$$\{y_{\mathrm{st}}\}=\begin{Bmatrix}u_v\\su_v\\s^2u_v+[\phi_{vc}]\,s^2\delta_c\end{Bmatrix}$$

$$\{y_a\}=\left\{u_{v_a}+\Big[\phi_{v_ac}\Big]\delta_c+\frac{1}{V}\Big[\phi_{v_aG}\Big]w_G\right\}\tag{7}$$

The term $[\phi_{vc}]s^2\delta_c$ appears in the third component of the vector $\{y_{\mathrm{st}}\}$ when the structural model of control surfaces contains the degrees of freedom involved in the mass variation. Similarly, the term $[\phi_{v_ac}]\delta_c$ appears in the vector $\{y_a\}$ when the degrees of freedom of the control surfaces are included into the aerodynamic variation, whereas the third term of the vector $\{y_a\}$ is required for gust response analysis of the perturbed system.

Express the model of Eqs. (3–5) as a system of linear first-order equations similar to the state-space form

$$\begin{aligned}s\{x_{\mathrm{ae}}\}&=[A_{\mathrm{ae}}(s)]\{x_{\mathrm{ae}}\}+\Big[B^{\mathrm{ae}}_{\mathrm{ae}}(s)\Big]\{u_{\mathrm{ae}}\}+\Big[B^{w}_{\mathrm{ae}}(s)\Big]\{w_G\}\\&\quad+\Big[B^{\mathrm{st}}_{\mathrm{ae}}\Big]\{u_{\mathrm{st}}\}+\Big[B^{a}_{\mathrm{ae}}\Big]\{u_a\}\end{aligned}\tag{8}$$

$$\begin{aligned}\{y_{\mathrm{ae}}\}&=[C_{\mathrm{ae}}(s)]\{x_{\mathrm{ae}}\}+\Big[D^{\mathrm{ae}}_{\mathrm{ae}}(s)\Big]\{u_{\mathrm{ae}}\}+\Big[D^{w}_{\mathrm{ae}}(s)\Big]\{w_G\}\\&\quad+\Big[D^{\mathrm{st}}_{\mathrm{ae}}\Big]\{u_{\mathrm{st}}\}+\Big[D^{a}_{\mathrm{ae}}\Big]\{u_a\}\end{aligned}\tag{9}$$

$$\begin{aligned}\{y_{\mathrm{st}}\}&=[C_{\mathrm{st}}(s)]\{x_{\mathrm{ae}}\}+\Big[D^{\mathrm{ae}}_{\mathrm{st}}(s)\Big]\{u_{\mathrm{ae}}\}+\Big[D^{w}_{\mathrm{st}}(s)\Big]\{w_G\}\\&\quad+\Big[D^{\mathrm{st}}_{\mathrm{st}}\Big]\{u_{\mathrm{st}}\}+\Big[D^{a}_{\mathrm{st}}\Big]\{u_a\}\end{aligned}\tag{10}$$

$$\begin{aligned}\{y_a\}&=[C_a]\{x_{\mathrm{ae}}\}+\Big[D^{\mathrm{ae}}_{a}\Big]\{u_{\mathrm{ae}}\}+\Big[D^{w}_{a}\Big]\{w_G\}\\&\quad+\Big[D^{\mathrm{st}}_{a}\Big]\{u_{\mathrm{st}}\}+\Big[D^{a}_{a}\Big]\{u_a\}\end{aligned}\tag{11}$$

$$\{u_{\mathrm{st}}\}=\bar{\Delta}_{\mathrm{st}}\{y_{\mathrm{st}}\}\tag{12}$$

$$\{u_a\}=\bar{\Delta}_a(s)\{y_a\}\tag{13}$$

where $\{y_{\mathrm{ae}}\}$ is the vector of output variables consisting of the measured structural displacements, velocities, and accelerations,

$$\{x_{\mathrm{ae}}\}=\begin{Bmatrix}\xi\\s\xi\end{Bmatrix},\qquad \{u_{\mathrm{ae}}\}=\begin{Bmatrix}\delta_c\\s\delta_c\\s^2\delta_c\end{Bmatrix}$$

$$[A_{\mathrm{ae}}(s)]=\begin{bmatrix}0&[I]\\-[M_{hh}]^{-1}[K_{hh}+qQ_{hh}(s)]&-[M_{hh}]^{-1}[B_{hh}]\end{bmatrix}$$

$$\Big[B^{\mathrm{ae}}_{\mathrm{ae}}(s)\Big]=\begin{bmatrix}0&0&0\\-q[M_{hh}]^{-1}[Q_{hc}(s)]&0&-[M_{hh}]^{-1}[M_{hc}]\end{bmatrix}$$

$$\Big[B^{w}_{\mathrm{ae}}(s)\Big]=\begin{bmatrix}0\\-\dfrac{q}{V}[M_{hh}]^{-1}[Q_{hG}(s)]\end{bmatrix}$$

$$[C_{\mathrm{ae}}(s)]=\begin{bmatrix}\Big[\phi_{y_1h}\Big]&0\\0&\Big[\phi_{y_2h}\Big]\\\Big[\phi_{y_3h}\Big]\Big[A^{(21)}_{\mathrm{ae}}\Big]&\Big[\phi_{y_3h}\Big]\Big[A^{(22)}_{\mathrm{ae}}\Big]\end{bmatrix}$$

$$\Big[B^{\mathrm{st}}_{\mathrm{ae}}\Big]=\begin{bmatrix}0\\\bar{B}^{\mathrm{st}}_{\mathrm{ae}}\end{bmatrix}[\Phi_{vh}]^T,\qquad \Big[B^{a}_{\mathrm{ae}}\Big]=\begin{bmatrix}0\\\bar{B}^{a}_{\mathrm{ae}}\end{bmatrix}\Big[\phi_{r_ah}\Big]^T$$

$$\Big[D^{\mathrm{ae}}_{\mathrm{ae}}(s)\Big]=\begin{bmatrix}0\\0\\\Big[\phi_{y_3h}\Big]\Big[B^{ae(2)}_{\mathrm{ae}}\Big]\end{bmatrix},\qquad \Big[D^{w}_{\mathrm{ae}}(s)\Big]=\begin{bmatrix}0\\0\\\Big[\phi_{y_3h}\Big]\Big[B^{w(2)}_{\mathrm{ae}}\Big]\end{bmatrix}$$

$$\Big[D^{\mathrm{st}}_{\mathrm{ae}}\Big]=\begin{bmatrix}0\\0\\\Big[\phi_{y_3h}\Big]\Big[\bar{B}^{\mathrm{st}}_{\mathrm{ae}}\Big]\end{bmatrix}[\Phi_{vh}]^T$$

$$\Big[D^{a}_{\mathrm{ae}}\Big]=\begin{bmatrix}0\\0\\\Big[\phi_{y_3h}\Big]\Big[\bar{B}^{a}_{\mathrm{ae}}\Big]\end{bmatrix}\Big[\phi_{r_ah}\Big]^T$$

$$\Big[C_{\mathrm{st}}(s)\Big]=[\Phi_{vh}]\begin{bmatrix}I_h&0\\0&I_h\\A^{(21)}_{\mathrm{ae}}&A^{(22)}_{\mathrm{ae}}\end{bmatrix}$$

$$\left[D^{\text{ae}}_{\text{st}}(s)\right] = \begin{bmatrix} 0 & 0 & 0 \\ 0 & 0 & 0 \\ \phi_{vh} B^{\text{ae}(21)}_{\text{ae}} & \phi_{vh} B^{\text{ae}(22)}_{\text{ae}} & \phi_{vh} B^{\text{ae}(23)}_{\text{ae}} + \phi_{vc} \end{bmatrix}$$

$$\left[D^{w}_{\text{st}}(s)\right] = [\Phi_{vh}] \begin{bmatrix} 0 \\ 0 \\ B^{w(2)}_{\text{ae}} \end{bmatrix}, \qquad \left[D^{\text{st}}_{\text{st}}\right] = [\Phi_{vh}] \begin{bmatrix} 0 \\ 0 \\ \bar{B}^{\text{st}}_{\text{ae}} \end{bmatrix} [\Phi_{vh}]^T$$

$$\left[D^{a}_{\text{st}}\right] = [\Phi_{vh}] \begin{bmatrix} 0 \\ 0 \\ \bar{B}^{a}_{\text{ae}} \end{bmatrix} \left[\phi_{r_a h}\right]^T$$

$$[C_a] = \left[\phi_{v_a h}\right][I_h \quad 0], \qquad \left[D^{\text{ae}}_{a}\right] = \left[\phi_{v_a c}\right][I_c \quad 0 \quad 0]$$

$$\left[D^{w}_{a}\right] = \left[\phi_{v_a G}\right], \qquad \left[D^{\text{st}}_{a}\right] = 0, \qquad \left[D^{a}_{a}\right] = 0$$

$$[\Phi_{vh}] = \text{diag}(\phi_{vh}, \phi_{vh}, \phi_{vh}), \; \bar{B}^{\text{st}}_{\text{ae}} = -[M_{hh}]^{-1}[I_h \quad I_h \quad I_h]$$

$$\bar{B}^{a}_{\text{ae}} = -q[M_{hh}]^{-1}$$

and where $[\phi_{y_1 h}]$, $[\phi_{y_2 h}]$, and $[\phi_{y_3 h}]$ are the normal modes for degrees of freedom prescribed for displacements, velocities, and accelerations measurements; $[A^{(ij)}_{\text{ae}}]$ are the blocks of the matrix $[A_{\text{ae}}]$; $[B^{**(2)}_{\text{ae}}]$ is the second block-row of the matrix $[B^{**}_{\text{ae}}]$; and I_h is the $n_h \times n_h$, unity matrix.

Rewrite Eqs. (8–11) in the form

$$s\{x_{\text{ae}}\} = [A_{\text{ae}}(s)]\{x_{\text{ae}}\} + \left[B^{\text{ae}}_{\text{ae}}(s)\right]\{u_{\text{ae}}\} + \left[B^{w}_{\text{ae}}(s)\right]\{w_G\} + \left[B^{\delta}_{\text{ae}}\right]\{u_\delta\} \tag{14}$$

$$\{y_{\text{ae}}\} = [C_{\text{ae}}(s)]\{x_{\text{ae}}\} + \left[D^{\text{ae}}_{\text{ae}}(s)\right]\{u_{\text{ae}}\} + \left[D^{w}_{\text{ae}}(s)\right]\{w_G\} + \left[D^{\delta}_{\text{ae}}\right]\{u_\delta\} \tag{15}$$

$$\{y_\delta\} = [C_\delta(s)]\{x_{\text{ae}}\} + \left[D^{\text{ae}}_{\delta}(s)\right]\{u_{\text{ae}}\} + \left[D^{w}_{\delta}(s)\right]\{w_G\} + \left[D^{\delta}_{\delta}\right]\{u_\delta\} \tag{16}$$

$$\{u_\delta\} = \bar{\Delta}(s)\{y_\delta\} \tag{17}$$

where

$$\{u_\delta\} = \begin{Bmatrix} u_{\text{st}} \\ u_a \end{Bmatrix}, \qquad \{y_\delta\} = \begin{Bmatrix} y_{\text{st}} \\ y_a \end{Bmatrix}$$

$$\bar{\Delta} = \text{diag}(\bar{\Delta}_{\text{st}}, \bar{\Delta}_a), \qquad \left[B^{\delta}_{\text{ae}}\right] = \left[B^{\text{st}}_{\text{ae}} \quad B^{a}_{\text{ae}}\right]$$

$$D^{\delta}_{\text{ae}} = \left[D^{\text{st}}_{\text{ae}} \quad D^{a}_{\text{ae}}\right], \qquad C_\delta(s) = \begin{bmatrix} C_{\text{st}} \\ C_a \end{bmatrix}, \qquad D^{\text{ae}}_{\delta}(s) = \begin{bmatrix} D^{\text{ae}}_{\text{st}} \\ D^{a}_{a} \end{bmatrix}$$

$$D^{w}_{\delta}(s) = \begin{bmatrix} D^{w}_{\text{st}} \\ D^{w}_{a} \end{bmatrix}, \qquad D^{\delta}_{\delta} = \begin{bmatrix} D^{\text{st}}_{\text{st}} & D^{a}_{\text{st}} \\ D^{\text{st}}_{a} & D^{a}_{a} \end{bmatrix}$$

The transfer matrix of the system governed by Eqs. (14–16) with the loop of the $\bar{\Delta}$ opened can be written as

$$\bar{P}(s) = \left[\begin{array}{c|ccc} A_{\text{ae}}(s) & B^{\delta}_{\text{ae}} & B^{w}_{\text{ae}}(s) & B^{\text{ae}}_{\text{ae}}(s) \\ \hline C_\delta(s) & D^{\delta}_{\delta} & D^{w}_{\delta}(s) & D^{\text{ae}}_{\delta}(s) \\ C_{\text{ae}}(s) & D^{\delta}_{\text{ae}} & D^{w}_{\text{ae}}(s) & D^{\text{ae}}_{\text{ae}}(s) \end{array}\right] \tag{18}$$

where

$$\left[\begin{array}{c|c} A(s) & B(s) \\ \hline C(s) & D(s) \end{array}\right] = [C(s)][s[I] - [A(s)]]^{-1}[B(s)] + [D(s)]$$

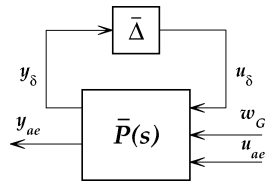

Fig. 1 LFT model of perturbed aeroelastic system.

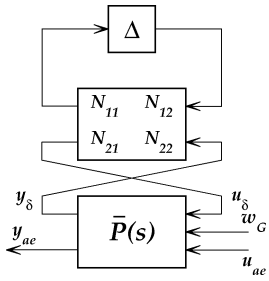

Fig. 2 Aeroelastic system with normalized variation.

The model of the perturbed aeroelastic system is obtained by closing of the $\bar{\Delta}$ loop as shown in Fig. 1. The transfer matrix of this system is expressed as

$$\bar{P}_{\bar{\Delta}}(s) = \mathcal{F}_u(\bar{P}, \bar{\Delta}) \tag{19}$$

where $\mathcal{F}_u(\cdot, \cdot)$ is the notation of an upper LFT.

IV. Models with Normalized Variations

Most problems require models incorporating nondimensional normalized variations or uncertainties. The expression relating absolute $\bar{\Delta}$ and normalized Δ variations may be cast as

$$\bar{\Delta} = \bar{\Delta}_0 + W_s W_l \Delta W_r \tag{20}$$

where $\bar{\Delta}_0$ is the fixed part of the absolute variation that is added to the baseline matrices and is not a subject of consequent perturbation analysis, W_s is the scaling matrix defining the maximal perturbation, and Δ is the $n_\Delta \times m_\Delta$ norm-bounded matrix of the normalized variation.

Dimensions of the absolute and normalized variations may be different. For example, if the matrix $\bar{\Delta}$ is a 2×2 stiffness (mass or damping) matrix of a scalar structural element, then the normalized variation can be presented as a scalar, whereas W_l and W_r become 2×1 and 1×2 matrices. As defined earlier, the matrices of the aerodynamic variations are rectangular and Eq. (20) enables one to express the normalized aerodynamic variation as a $n_{v_a} \times n_{v_a}$ square matrix. In these cases, the dimension of the square matrix Δ is equal to the rank of the matrix $\bar{\Delta}$.

Equation (20) can be written in a more general form as an LFT:

$$\bar{\Delta} = \mathcal{F}_u(N, \Delta) \tag{21}$$

where N is the $(n_{\bar{\Delta}} + m_\Delta) \times (m_{\bar{\Delta}} + n_\Delta)$ LFT matrix and $n_{\bar{\Delta}}$ and $m_{\bar{\Delta}}$ are the numbers of rows and columns of the matrix $\bar{\Delta}$.

Equation (21) enables one to construct models of perturbed ASE systems incorporating variations of so-called structural design variables of the system, such as geometrical and inertial parameters of structural elements, material properties, etc. The LFT presentation of the matrix $\bar{\Delta}$ enables modeling of nonlinear dependence of the matrix $\bar{\Delta}$ on variations of design variables, for example, positions of centers of gravity of lumped mass elements. The normalized variation of Eq. (20) is obtained from the LFT presentation of Eq. (21) when $N_{11} = 0$, $N_{12} = W_r$, $N_{21} = W_s W_l$, and $N_{22} = \bar{\Delta}_0$.

Augmentation of Eq. (21) into the model of Eqs. (14–16) is expressed graphically in Fig. 2. Performing elementary LFT operations obtains the the transfer matrix of the augmented aeroelastic system as

$$P(s) = \begin{bmatrix} N_{11} + N_{12} L_1 \bar{P}_{11} N_{21} & N_{12} L_1 \bar{P}_{12} \\ \bar{P}_{21} L_2 N_{21} & \bar{P}_{22} + \bar{P}_{21} L_2 N_{22} \bar{P}_{12} \end{bmatrix} \tag{22}$$

where $\bar{P}_{ij}$ are the partitions of the transfer matrix $\bar{P}$, $L_1 = (I - N_{11}\bar{P}_{22})$, and $L_2 = (I - N_{22}\bar{P}_{11})$.

V. Closed-Loop ASE System with Structural and Aerodynamic Variations

The model of the closed-loop ASE system contains the equations of motion of the open-loop aeroelastic system accomplished with the state-space model of the actuators and with the state-space representation of the linear time-invariant controller.[8]

Augmentation of the open-loop aeroelastic model (14–16) with the model of the actuators leads to equations of the perturbed ASE plant:

$$s\{x_p\} = [A_p(s)]\{x_p\} + \left[B_p^p\right]\{u_p\} + \left[B_p^w(s)\right]\{w_G\} + \left[B_p^\delta\right]\{u_\delta\} \quad (23)$$

$$\{y_p\} = [C_p(s)]\{x_p\} + \left[D_p^p\right]\{u_p\} + \left[D_p^w(s)\right]\{w_G\} + \left[D_p^\delta\right]\{u_\delta\} \quad (24)$$

$$\{y_\delta\} = \left[C_\delta^p(s)\right]\{x_p\} + \left[D_\delta^p\right]\{u_p\} + \left[D_\delta^w(s)\right]\{w_G\} + \left[D_\delta^\delta\right]\{u_\delta\} \quad (25)$$

where $\{u_p\}$ is the vector of n_c actuator inputs and $\{y_p\} = \{y_{\text{ae}}\}$ is the vector of sensor signals. The vector of the plant states $\{x_p\}$ includes the vectors $\{x_{\text{ae}}\}$ and $\{u_{\text{ae}}\}$ and the vector of actuator states $\{x_{\text{ac}}\}$, and so the model matrices are expressed as

$$[A_p(s)] = \begin{bmatrix} A_{\text{ae}} & B_{\text{ae}} \\ 0 & A_{\text{ac}} \end{bmatrix}, \qquad \left[B_p^p\right] = \begin{bmatrix} 0 \\ B_{\text{ac}} \end{bmatrix}, \qquad \left[B_p^w(s)\right] = \begin{bmatrix} B_{\text{ae}}^w \\ 0 \end{bmatrix}$$

$$[C_p(s)] = \begin{bmatrix} C_{\text{ae}} & D_{\text{ae}}^{\text{ae}} \end{bmatrix}, \qquad \left[D_p^w(s)\right] = \left[D_{\text{ae}}^w\right], \qquad \left[D_p^p\right] = 0$$

$$\left[B_p^\delta\right] = \begin{bmatrix} B_{\text{ae}}^\delta \\ 0 \end{bmatrix}, \qquad \left[D_p^\delta\right] = \left[D_{\text{ae}}^\delta\right]$$

$$\left[C_\delta^p(s)\right] = \begin{bmatrix} C_\delta^{\text{ae}} & D_\delta^{\text{ae}} \end{bmatrix}, \qquad \left[D_\delta^p\right] = 0$$

where the matrices $[A_{\text{ac}}]$ and $[B_{\text{ac}}]$ incorporate the actuator dynamics modeled by

$$s\{x_{\text{ac}}\} = [A_{\text{ac}}]\{x_{\text{ac}}\} + [B_{\text{ac}}]\{u_p\} \quad (26)$$

Third-order actuator dynamics is assumed. Higher-order actuator dynamics and the sensor dynamics can be included as parts of the control system. (See Ref. 8 for details.)

The model of the perturbed closed-loop ASE system is obtained by augmenting the plant model of Eqs. (23–25) with the model of the linear controller defined by its state-space matrices $[A_c]$, $[B_c]$, $[C_c]$, and $[D_c]$. The uncoupled plant and control equations are expressed as

$$s\{x_V\} = [A_V(s)]\{x_V\} + \left[B_V^V\right]\{u_V\} + \left[B_V^w(s)\right]\{w_G\} + \left[B_V^\delta\right]\{u_\delta\} \quad (27)$$

$$\{y_V\} = [C_V(s)]\{x_V\} + \left[D_V^V\right]\{u_V\} + \left[D_V^w(s)\right]\{w_G\} + \left[D_V^\delta\right]\{u_\delta\} \quad (28)$$

$$\{y_\delta\} = \left[C_\delta^V(s)\right]\{x_V\} + \left[D_\delta^V\right]\{u_V\} + \left[D_\delta^w(s)\right]\{w_G\} + \left[D_\delta^\delta\right]\{u_\delta\} \quad (29)$$

where

$$\{x_V\} = \begin{Bmatrix} x_p \\ x_c \end{Bmatrix}, \qquad \{u_V\} = \begin{Bmatrix} u_p \\ u_c \end{Bmatrix}, \qquad \{y_V\} = \begin{Bmatrix} y_p \\ y_c \end{Bmatrix}$$

and where $\{x_c\}$, $\{u_c\}$, and $\{y_c\}$ are the vectors of controller states, inputs, and outputs,

$$[A_V(s)] = \begin{bmatrix} A_p & 0 \\ 0 & A_c \end{bmatrix}, \qquad \left[B_V^V\right] = \begin{bmatrix} B_p^p & 0 \\ 0 & B_c \end{bmatrix}$$

$$\left[B_V^w(s)\right] = \begin{bmatrix} B_p^w \\ 0 \end{bmatrix}, \qquad \left[B_V^\delta\right] = \begin{bmatrix} B_p^\delta \\ 0 \end{bmatrix}$$

$$[C_V(s)] = \begin{bmatrix} C_p & 0 \\ 0 & C_c \end{bmatrix}, \qquad \left[D_V^V\right] = \begin{bmatrix} D_p^p & 0 \\ 0 & D_c \end{bmatrix}$$

$$\left[D_V^w(s)\right] = \begin{bmatrix} D_p^w \\ 0 \end{bmatrix}, \qquad \left[D_V^\delta\right] = \begin{bmatrix} D_p^\delta \\ 0 \end{bmatrix}$$

$$\left[C_\delta^V(s)\right] = \begin{bmatrix} C_\delta^p & 0 \end{bmatrix}, \qquad \left[D_\delta^V\right] = \begin{bmatrix} D_\delta^p & 0 \end{bmatrix}$$

The ASE loop is closed by the output feedback $\{u_V\} = [G_{VV}]\{y_V\}$ leading to the resulting closed-loop ASE equations of motion for the perturbed system:

$$s\{x_V\} = [A_{\text{ase}}]\{x_V\} + \left[B_{\text{ase}}^w\right]\{w_G\} + \left[B_{\text{ase}}^\delta\right]\{u_\delta\} \quad (30)$$

$$\{y_\delta\} = \left[C_\delta^{\text{ase}}\right]\{x_V\} + \left[\mathcal{D}_\delta^w\right]\{w_G\} + \left[\mathcal{D}_\delta^\delta\right]\{u_\delta\} \quad (31)$$

where

$$[A_{\text{ase}}(s)] = \mathcal{F}_\ell\left(\begin{bmatrix} A_V & B_V^V \\ C_V & D_V^V \end{bmatrix}, G_{VV}\right)$$

$$\left[B_{\text{ase}}^w(s)\right] = \mathcal{F}_\ell\left(\begin{bmatrix} B_V^w & B_V^V \\ D_V^w & D_V^V \end{bmatrix}, G_{VV}\right)$$

$$\left[B_{\text{ase}}^\delta\right] = \mathcal{F}_\ell\left(\begin{bmatrix} B_V^\delta & B_V^V \\ D_V^\delta & D_V^V \end{bmatrix}, G_{VV}\right)$$

$$\left[C_\delta^{\text{ase}}(s)\right] = \mathcal{F}_\ell\left(\begin{bmatrix} C_\delta^V & D_\delta^V \\ C_V & D_V^V \end{bmatrix}, G_{VV}\right)$$

$$\left[\mathcal{D}_\delta^w(s)\right] = \mathcal{F}_\ell\left(\begin{bmatrix} D_\delta^w & D_\delta^V \\ D_V^w & D_V^V \end{bmatrix}, G_{VV}\right)$$

$$\left[\mathcal{D}_\delta^\delta\right] = \mathcal{F}_\ell\left(\begin{bmatrix} D_\delta^\delta & D_\delta^V \\ D_V^\delta & D_V^V \end{bmatrix}, G_{VV}\right)$$

Augmentation of the obtained model of Eqs. (30) and (31) with Eq. (21) leads to the model of the perturbed closed-loop ASE system with normalized uncertainty.

VI. Variation Models in Generalized Coordinates

The presented modeling technique enables constructing LFT models of the perturbed ASE systems so that the structural and aerodynamic variations are incorporated into the model in discrete form without transformations to the modal coordinates. This is important for the modeling of the local structural and/or aerodynamic variations when the number of discrete degrees of freedom involved in the variation is less than the number of modes applied in the analysis. In this case, the variation modeling in discrete coordinates leads to minimal dimension of the uncertainty matrices.

Application of the variation models defined in the generalized coordinates may be preferable when the number of discrete degrees of freedom involved in the variation (n_v or n_{v_a}) is greater than the number of modes. In this case, the modal presentation decreases the size of the variation matrices with respect to the discrete-coordinates models. The model of the perturbed aeroelastic system with the modal variation matrices can be obtained from the model of Eqs. (8–11) by moving the terms $[\Phi_{vh}]^T$ and $[\phi_{v_a h}]^T$ from all of the matrices with the superscripts st and a to the matrices of the absolute variations $\bar{\Delta}_{\text{st}}$ and $\bar{\Delta}_a$. This leads to the matrices $\bar{\Delta}_{\text{st}}$ and $\bar{\Delta}_a$ of dimensions $3n_h \times 3n_v$ and $n_h \times n_{v_a}$, respectively. Then the resulting normalized variation Δ of Eq. (20) or (21) becomes of dimension $(3n_h + n_h) \times (3n_h + n_h)$.

VII. State-Space Model of Perturbed ASE System

The models in the Laplace domain developed in the preceding sections enables one to perform analysis of the ASE systems in

the frequency domain by replacing s by $i\omega$. Some tasks such as a modern robust control design require state-space models of the perturbed open-loop ASE systems to be constructed. These kinds of models are based on the rational approximation of the unsteady generalized aerodynamic force matrices, in the Laplace domain, of the form (see Refs. 8 and 9)

$$[\tilde{Q}_h(s)] = [A_{h0}] + (b/V)[A_{h1}]s + (b^2/V^2)[A_{h2}]s^2 + [D_h]([I]s - (V/b)[R])^{-1}[E]s \tag{32}$$

where the $[A_{hi}]$ and $[E]$ approximation matrices are column partitioned according to the structural, control, and gust modes as

$$\left[A_{h_i}\right] = \left[A_{hh_i} \quad A_{hc_i} \quad A_{hG_i}\right] \qquad (i = 0, 1, 2)$$

$$[E] = [E_h \quad E_c \quad E_G]$$

The real coefficient matrices in Eq. (32) are determined in a nonlinear least-square solution that approximates a set of generalized force coefficients matrices $[Q_h(ik)]$ (Refs. 9 and 10).

The state-space model of the perturbed aeroelastic system is obtained from the Laplace-domain model of Eqs. (8–11) performing the rational approximation of the aerodynamic matrices $[Q_{hh}]$, $[Q_{hc}]$, and $[Q_{hG}]$. Observe that the matrices of the Laplace-domain model corresponding to the feedback (variation) inputs $\{u_{\rm st}\}$ and $\{u_a\}$, that is, matrices B and D with the superscripts st and a, are not the functions of the Laplace variable s and they are not involved in the approximation process. Therefore, the state-space modeling procedure developed in Refs. 9 and 10 can be directly applied for converting the Laplace-domain model of Eqs. (8–11) to the state-space representation. To accomplish the modeling process, the frequency-dependent aerodynamic variation $\bar{\Delta}_a(s)$ should be presented in the state-space using rational approximation of the matrix $[\mathrm{AIC}_{r_a v_a}(s)]$:

$$\left[\widetilde{\mathrm{AIC}}_{r_a v_a}\right] = \left[A_{r_a v_a,0}\right] + (b/V)\left[A_{r_a v_a,1}\right]s + (b^2/V^2)\left[A_{r_a v_a,2}\right]s^2 + \left[D_{r_a}\right]([I]s - (V/b)[R_\Delta])^{-1}\left[E_{v_a}\right]s \tag{33}$$

where $[A_{r_a v_a,i}]$, $[D_{r_a}]$, $[E_{v_a}]$, and $[R_\Delta]$ are the aerodynamic approximation matrices.

This approximation results in the state-space representation of the product $[\widetilde{\mathrm{AIC}}_{r_a v_a}]\{u_{v_a}\}$:

$$\{\dot{x}_{a\Delta}\} = [A_{a\Delta}]\{x_{a\Delta}\} + [B_{a\Delta}]\{y_a\} + [B_{a\Delta}]\left[\Phi_{v_a c}\right]\{u_{\rm ae}\} + [B_{a\Delta}]\left[\Phi_{v_a G}\right]\{\bar{w}_G\} \tag{34}$$

$$\left[\widetilde{\mathrm{AIC}}_{r_a v_a}\right]\left\{u_{v_a}\right\} = [C_{a\Delta}]\{x_{a\Delta}\} + [D_{a\Delta}]\{y_a\} + [D_{a\Delta}]\left[\Phi_{v_a c}\right]\{u_{\rm ae}\} + [D_{a\Delta}]\left[\Phi_{v_a G}\right]\{\bar{w}_G\} \tag{35}$$

where

$$\{y_a\} = \begin{Bmatrix} u_{v_a} \\ \dot{u}_{v_a} \\ \ddot{u}_{v_a} \end{Bmatrix}, \qquad \{u_{\rm ae}\} = \begin{Bmatrix} \delta_c \\ \dot{\delta}_c \\ \ddot{\delta}_c \end{Bmatrix}, \qquad \{\bar{w}_G\} = \begin{Bmatrix} w_G \\ \dot{w}_G \\ \ddot{w}_G \end{Bmatrix}$$

$$[A_{a\Delta}] = (V/b)[R_\Delta], \qquad [B_{a\Delta}] = [0 \quad E_{v_a} \quad 0], \qquad [C_{a\Delta}] = q\left[D_{r_a}\right]$$

$$[D_{a\Delta}] = \left[q A_{r_a v_a,0} \quad (qb/V) A_{r_a v_a,1} \quad (qb^2/V^2) A_{r_a v_a,2}\right]$$

$$\left[\Phi_{v_a c}\right] = \mathrm{diag}\left(\phi_{v_a c}, \phi_{v_a c}, \phi_{v_a c}\right)$$

$$\left[\Phi_{v_a G}\right] = \mathrm{diag}\left(\phi_{v_a G}, \phi_{v_a G}, \phi_{v_a G}\right)$$

Express Eq. (3) in time domain using the aerodynamic approximation of Eq. (32) for the nominal system and the approximation of Eqs. (34) and (35) for the aerodynamic variation $\bar{\Delta}_a(s)$:

$$[\bar{M}_{hh}]\{\ddot{\xi}\} + [\bar{K}_{hh} \quad \bar{B}_{hh} \quad qD_h]\{x_{\rm ae}\} = -[\bar{K}_{hc} \quad \bar{B}_{hc} \quad \bar{M}_{hc}]\{u_{\rm ae}\} - [\bar{K}_{hG} \quad \bar{B}_{hG} \quad \bar{M}_{hG}]\{\bar{w}_G\} - [\phi_{vh}]^T[K_{vv} \quad B_{vv} \quad M_{vv}]\{y_{\rm st}\} - \left[\phi_{r_a h}\right]^T[C_{a\Delta}]\{x_{a\Delta}\} - \left[\phi_{r_a h}\right]^T[D_{a\Delta}]\{y_a\} - \left[\phi_{r_a h}\right]^T[D_{a\Delta}]\left[\Phi_{v_a c}\right]\{u_{\rm ae}\} - \left[\phi_{r_a h}\right]^T[D_{a\Delta}]\left[\Phi_{v_a G}\right]\{\bar{w}_G\} \tag{36}$$

where

$$\{x_{\rm ae}\} = \begin{Bmatrix} \xi \\ \dot{\xi} \\ x_a \end{Bmatrix}, \qquad \{y_{\rm st}\} = \begin{Bmatrix} u_v \\ \dot{u}_v \\ \ddot{u}_v + \phi_{vc}\ddot{\delta}_c \end{Bmatrix}$$

$$[\bar{M}_{hh}] = [M_{hh}] + (qb^2/V^2)\left[A_{hh_2}\right], \qquad [\bar{K}_{hh}] = [K_{hh}] + q\left[A_{hh_0}\right]$$

$$[\bar{B}_{hh}] = [B_{hh}] + (qb/V)\left[A_{hh_1}\right]$$

$$[\bar{K}_{hc}] = q\left[A_{hc_0}\right], \qquad [\bar{B}_{hc}] = (qb/V)\left[A_{hc_1}\right]$$

$$[\bar{M}_{hc}] = [M_{hc}] + (qb^2/V^2)\left[A_{hc_2}\right]$$

$$[\bar{K}_{hG}] = (q/V)\left[A_{hG_0}\right], \qquad [\bar{B}_{hG}] = (qb/V^2)\left[A_{hG_1}\right]$$

$$[\bar{M}_{hG}] = (qb^2/V^3)\left[A_{hG_2}\right]$$

To eliminate the second time derivative $\ddot{w}_g$ of the gust velocity, approximation constraints for the nominal system should be applied to yield $[A_{hG_2}] = 0$, and, therefore, $[\bar{M}_{hG}] = 0$. (See Ref. 10 for details.) Similar approximation constraints $[A_{r_a v_a,2}]\{\phi_{v_a G}\} = 0$ should be applied for the aerodynamic variation.

Equations (34–36) lead to the state-space model of aeroelastic system with the state-space representation of aerodynamic variation:

$$\{\dot{x}_{\rm ae}\} = [A_{\rm ae}]\{x_{\rm ae}\} + \left[B^{\rm ae}_{\rm ae}\right]\{u_{\rm ae}\} + \left[B^{w}_{\rm ae}\right]\{w_G\} + \left[B^{\rm st}_{\rm ae}\right]\{u_{\rm st}\} + \left[B^{a}_{\rm ae}\right]\{u_a\} \tag{37}$$

$$\{y_{\rm ae}\} = [C_{\rm ae}]\{x_{\rm ae}\} + \left[D^{\rm ae}_{\rm ae}\right]\{u_{\rm ae}\} + \left[D^{w}_{\rm ae}\right]\{w_G\} + \left[D^{\rm st}_{\rm ae}\right]\{u_{\rm st}\} + \left[D^{a}_{\rm ae}\right]\{u_a\} \tag{38}$$

$$\{y_{\rm st}\} = [C_{\rm st}]\{x_{\rm ae}\} + \left[D^{\rm ae}_{\rm st}\right]\{u_{\rm ae}\} + \left[D^{w}_{\rm st}\right]\{w_G\} + \left[D^{\rm st}_{\rm st}\right]\{u_{\rm st}\} + \left[D^{a}_{\rm st}\right]\{u_a\} \tag{39}$$

$$\{y_a\} = [C_a]\{x_{\rm ae}\} + \left[D^{\rm ae}_{a}\right]\{u_{\rm ae}\} + \left[D^{w}_{a}\right]\{w_G\} + \left[D^{\rm st}_{a}\right]\{u_{\rm st}\} + \left[D^{a}_{a}\right]\{u_a\} \tag{40}$$

$$\{u_{\rm st}\} = \bar{\Delta}_{\rm st}\{y_{\rm st}\} \tag{41}$$

$$\{\dot{x}_{a\Delta}\} = [A_{a\Delta}]\{x_{a\Delta}\} + [B_{a\Delta}]\{y_a\} + [B_{a\Delta}]\left[\Phi_{v_a c}\right]\{u_{\rm ae}\} + [B_{a\Delta}]\left[\Phi_{v_a G}\right]\{\bar{w}_G\} \tag{42}$$

$$\{u_a\} = [C_{a\Delta}]\{x_{a\Delta}\} + [D_{a\Delta}]\{y_a\} + [D_{a\Delta}]\left[\Phi_{v_a c}\right]\{u_{\rm ae}\} + [D_{a\Delta}]\left[\Phi_{v_a G}\right]\{\bar{w}_G\} \tag{43}$$

where

$$[A_{\rm ae}] = \begin{bmatrix} 0 & [I] & 0 \\ -[\bar{M}_{hh}]^{-1}[\bar{K}_{hh}] & -[\bar{M}_{hh}]^{-1}[\bar{B}_{hh}] & -q[\bar{M}_{hh}]^{-1}[D_h] \\ 0 & [E_h] & (V/b)[R] \end{bmatrix}$$

$$\left[B_{\text{ae}}^{\text{ae}}\right]=\begin{bmatrix}0 & 0 & 0\\ -[\bar{M}_{hh}]^{-1}[\bar{K}_{hc}] & -[\bar{M}_{hh}]^{-1}[\bar{B}_{hc}] & -[\bar{M}_{hh}]^{-1}[\bar{M}_{hc}]\\ 0 & [E_c] & 0\end{bmatrix}$$

$$\left[B_{\text{ae}}^{w}\right]=\begin{bmatrix}0 & 0 & 0\\ -[\bar{M}_{hh}]^{-1}[\bar{K}_{hG}] & -[\bar{M}_{hh}]^{-1}[\bar{B}_{hG}] & -[\bar{M}_{hh}]^{-1}[\bar{M}_{hG}]\\ 0 & (1/V)[E_G] & 0\end{bmatrix}$$

$$[C_{\text{ae}}]=\begin{bmatrix}\left[\phi_{y_1h}\right] & 0 & 0\\ 0 & \left[\phi_{y_2h}\right] & 0\\ \left[\phi_{y_3h}\right]\left[A_{\text{ae}}^{(21)}\right] & \left[\phi_{y_3h}\right]\left[A_{\text{ae}}^{(22)}\right] & \left[\phi_{y_3h}\right]\left[A_{\text{ae}}^{23}\right]\end{bmatrix}$$

$$\left[D_{\text{ae}}^{\text{ae}}\right]=\begin{bmatrix}0\\ 0\\ \left[\phi_{y_3h}\right]\left[B_{\text{ae}}^{\text{ae}(2)}\right]\end{bmatrix},\qquad \left[D_{\text{ae}}^{w}\right]=\begin{bmatrix}0\\ 0\\ \left[\phi_{y_3h}\right]\left[B_{\text{ae}}^{w(2)}\right]\end{bmatrix}$$

$$\left[B_{\text{ae}}^{\text{st}}\right]=\begin{bmatrix}0\\ \bar{B}_{\text{ae}}^{\text{st}}\\ 0\end{bmatrix}[\Phi_{vh}]^T,\qquad \left[B_{\text{ae}}^{a}\right]=\begin{bmatrix}0\\ \bar{B}_{\text{ae}}^{a}\\ 0\end{bmatrix}\left[\phi_{r_ah}\right]^T$$

$$\left[D_{\text{ae}}^{\text{st}}\right]=\begin{bmatrix}0\\ 0\\ \left[\phi_{y_3h}\right]\left[\bar{B}_{\text{ae}}^{\text{st}}\right]\end{bmatrix}[\Phi_{vh}]^T$$

$$\left[D_{\text{ae}}^{a}\right]=\begin{bmatrix}0\\ 0\\ \left[\phi_{y_3h}\right]\left[\bar{B}_{\text{ae}}^{a}\right]\end{bmatrix}\left[\phi_{r_ah}\right]^T$$

$$[C_{\text{st}}]=[\Phi_{vh}]\begin{bmatrix}I_h & 0 & 0\\ 0 & I_h & 0\\ A_{\text{ae}}^{(21)} & A_{\text{ae}}^{(22)} & A_{\text{ae}}^{(23)}\end{bmatrix}$$

$$\left[D_{\text{st}}^{\text{ae}}\right]=\begin{bmatrix}0 & 0 & 0\\ 0 & 0 & 0\\ \phi_{vh}B_{\text{ae}}^{\text{ae}(21)} & \phi_{vh}B_{\text{ae}}^{\text{ae}(22)} & \phi_{vh}B_{\text{ae}}^{\text{ae}(23)}+\phi_{vc}\end{bmatrix}$$

$$\left[D_{\text{st}}^{w}\right]=[\Phi_{vh}]\begin{bmatrix}0\\ 0\\ B_{\text{ae}}^{w(2)}\end{bmatrix},\qquad \left[D_{\text{st}}^{\text{st}}\right]=[\Phi_{vh}]\begin{bmatrix}0\\ 0\\ \bar{B}_{\text{ae}}^{\text{st}}\end{bmatrix}[\Phi_{vh}]^T$$

$$\left[D_{\text{st}}^{a}\right]=[\Phi_{vh}]\begin{bmatrix}0\\ 0\\ -q[\bar{M}_{hh}]^{-1}\end{bmatrix}\left[\phi_{r_ah}\right]^T$$

$$[C_a]=\left[\Phi_{v_ah}\right]\begin{bmatrix}I_h & 0 & 0\\ 0 & I_h & 0\\ A_{\text{ae}}^{(21)} & A_{\text{ae}}^{(22)} & A_{\text{ae}}^{(23)}\end{bmatrix}$$

$$\left[D_{a}^{\text{ae}}\right]=\left[\Phi_{v_ah}\right]\begin{bmatrix}0\\ 0\\ B_{\text{ae}}^{\text{ae}(2)}\end{bmatrix},\qquad \left[D_{a}^{w}\right]=\left[\Phi_{v_ah}\right]\begin{bmatrix}0\\ 0\\ B_{\text{ae}}^{w(2)}\end{bmatrix}$$

$$\left[D_{a}^{\text{st}}\right]=\left[\Phi_{v_ah}\right]\begin{bmatrix}0\\ 0\\ \bar{B}_{\text{ae}}^{\text{st}}\end{bmatrix}[\Phi_{vh}]^T,\qquad \left[D_{a}^{a}\right]=\left[\Phi_{v_ah}\right]\begin{bmatrix}0\\ 0\\ \bar{B}_{\text{ae}}^{a}\end{bmatrix}\left[\phi_{r_ah}\right]^T$$

$$\left[\Phi_{v_ah}\right]=\operatorname{diag}\left(\phi_{v_ah},\phi_{v_ah},\phi_{v_ah}\right)$$

$$\bar{B}_{\text{ae}}^{\text{st}}=-[\bar{M}_{hh}]^{-1}[I_h\quad I_h\quad I_h],\qquad \bar{B}_{\text{ae}}^{a}=-q[\bar{M}_{hh}]^{-1}$$

To obtain the state-space model with the aerodynamic variation in generalized coordinates rewrite Eq. (3) as

$$\begin{aligned}&\left([M_{hh}]s^2+[B_{hh}]s+[K_{hh}]+q[Q_{hh}(s)]\right)\{\xi(s)\}\\ &\quad=-\left([M_{hc}]s^2+q[Q_{hc}(s)]\right)\{\delta_c(s)\}-(q/V)[Q_{hG}(s)]\{w_G(s)\}\\ &\quad-[\phi_{vh}]^T\left([M_{vv}]s^2+[B_{vv}]s+[K_{vv}]\right)\{u_v(s)\}\\ &\quad-[\phi_{vh}]^T[M_{vv}][\phi_{vc}]s^2\{\delta_c(s)\}\\ &\quad-q[\Delta Q_h(s)][\xi(s)\quad \delta_c(s)\quad (1/V)w_g(s)]^T\end{aligned}\tag{44}$$

where

$$\begin{aligned}[\Delta Q_h(s)]&=[\Delta Q_{hh}(s)\quad \Delta Q_{hc}(s)\quad \Delta Q_{hG}(s)]\\ &=\left[\phi_{r_ah}\right]^T\left[\text{AIC}_{r_av_a}(s)\right]\left[\phi_{v_ah}\quad \phi_{v_ac}\quad \phi_{v_aG}\right]\end{aligned}$$

The matrix $[\Delta Q_h(s)]$ is approximated exactly as the baseline aerodynamic matrix $[Q_h(s)]$. The state-space model incorporating the variation $[\Delta Q_h(s)]$ is obtained from Eqs. (37–43) by removing the terms $[\phi_{r_ah}]^T$ and $[\Phi_{v_ah}]$ from the matrices with the sub- and superscripts a of Eqs. (37–41) and by removing the terms $[\Phi_{v_ac}]$ and $[\Phi_{v_aG}]$ from Eqs. (42) and (43). The removed terms are inserted into the the matrix $[Q_h(s)]$ so they are taken into account in the aerodynamic approximation matrices.

VIII. Numerical Example

A. Test-Case ASE System

The preceding technique for aeroservoelastic modeling with structural and aerodynamic variations is demonstrated using the aeroelastic model of a UAV. The MacNeal Schwendler Corp. (MSC)/NASTRAN aircraft structural model of the UAV right-hand side is shown in Fig. 3. The weight of the model is 152 kg. The half-span of the wing is 4.0 m, and the uniform chord length is 0.55 m. The model contains 459 grid points and 580 structural elements leading to 2315 free degrees of freedom. The UAV unsteady aerodynamic model is shown in Fig. 4 with the locations of four

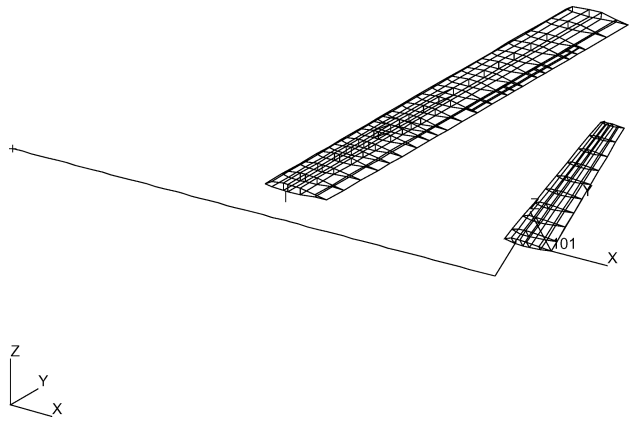

Fig. 3 UAV structural model.

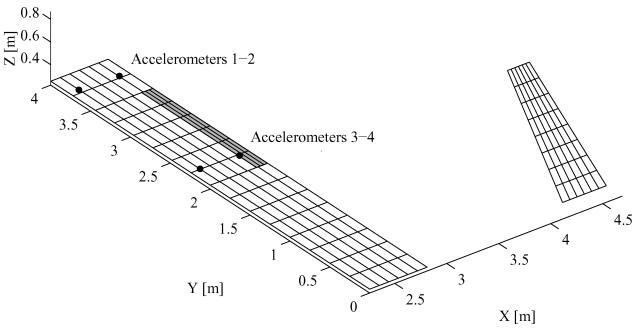

Fig. 4 UAV aerodynamic model.

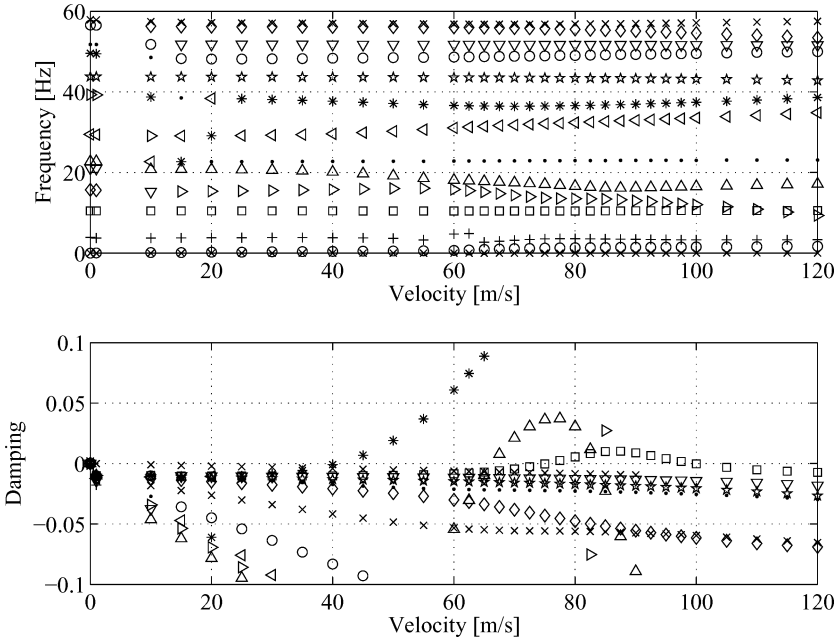

Fig. 5 Open-loop flutter analysis.

accelerometers for subsequent ASE analysis. The model consists of five aerodynamic panels representing the parts of the wing (three panels), aileron, and elevator–rudder. All of the panels are splined to the structural grid points. More details concerning the UAV models as well as the results of stability, dynamic response, and sensitivity analyses may be found in Ref. 11.

Normal modes analysis was performed with symmetric boundary conditions to extract the 14 lowest-frequency modes, including two rigid-body modes (heave and pitch), up to 58 Hz.

Open-loop flutter analysis at Mach 0.0 was performed with frequency-domain g-method using ZAERO software with MSC/NASTRAN aerodynamics. There were generalized aerodynamic force matrices at reduced frequency values between $k = 0.0001$ and $k = 3.6$ calculated by MSC/NASTRAN exported to ZAERO. Computation were performed at 32 velocity points spaced between 1.0 and 120.0 m/s. Structural damping of $g = 0.01$ was defined for all frequencies. The flutter analysis results, in terms of the variation with velocity of the frequency f and damping g values associated with the structural modes (V–g plots), are shown in Fig. 5. The V–g plots indicate four flutter mechanisms[11]: 1) control-surface flutter between the aileron mode and the third wing bending mode, $V_F = 40.57$ m/s and $f_F = 37.7$ Hz; 2) bending–torsion flutter between the torsion and the second wing bending modes, $V_F = 66.45$ m/s and $f_F = 17.7$ Hz; 3) very mild flutter between the torsion and fore-and-aft modes, $V_F = 75.26$ m/s and $f_F = 10.4$ Hz; and 4) classical explosive bending–torsion flutter with the first bending mode and the torsion mode, $V_F = 84.27$ m/s and $f_F = 13.4$ Hz. The most critical is the aileron-bending flutter with the lowest flutter velocity of 40.57 m/s.

The feedback control system was designed to suppress the instabilities of the open-loop aeroelastic system. The control system contains four acceleration sensors, robust μ controller, and the actuator of the wing control surface. (The aerodynamic panel representing the control surface is shaded in Fig. 4.) The third-order transfer function of the actuator was defined as

$$\frac{\delta_c(s)}{u_{\text{ac}}(s)} = \frac{6{,}751{,}689.0}{s^3 + 259.97s^2 + 66{,}157.39s + 6{,}751{,}689.0} \tag{45}$$

The μ controller was presented by the state-space model with 4 inputs, 1 output, and 35 states. It was designed to address the velocity variations and the uncertainties relating to unmodeled dynamics of the aeroelastic system. (For details, see Ref. 12.) The frequency-domain model of the closed-loop ASE system was obtained by augmentation of the frequency-domain model of the ASE plant with the state-space model of the controller. Stability analysis of the closed-loop ASE system performed using the g-method of ZAERO[7,13] indicates three ASE instabilities: 1) the control surface oscillations caused by the ASE interaction between the controller and the aileron (where the oscillations occur at velocities less than $V_F = 32.15$ m/s with the frequency $f_F = 54.5$ Hz); 2) flutter between the first bending mode and the control system dynamics, $V_F = 100.34$ m/s and $f_F = 3.1$ Hz; and 3) flutter between the third bending mode and the control system dynamics, $V_F = 107.80$ m/s and $f_F = 28.2$ Hz. Instabilities of the first and third mechanisms are shown in the V–g plots presented in Fig. 6. The second mechanism is outside the scale of the V–g plot because its damping changes from -0.165 to 2.245, whereas the velocity increases from 100.0 to 105.0 m/s.

B. Robust Stability Analysis

Suppressing the aeroelastic instabilities of the open-loop system the control system introduces new instabilities into the ASE system. The results of the open- and closed-loop stability analyses demonstrate that the open-loop aeroelastic system is stable in the velocity range from 0.0 to 40.57 m/s, whereas the closed-loop ASE system is stable in the range from 32.15 to 100.34 m/s. Therefore, a scheduled application, where the control system is turned on and off in the velocity range of 32.15–40.57 m/s, should be used in this case. The goal of the robust stability analysis is to evaluate the influence of uncertainties in the structural and aerodynamic parameters of the aileron on the range of overlap stability of the open- and closed-loop systems. The parameters of the control surface should be considered in the robust stability analysis because the velocity of the open-loop aileron flutter is critical for the range of stability and the aileron parameters are important for stability of the closed-loop system. The robust stability analysis is performed with respect to uncertainties in the aileron inertial properties and the AICs relating the aileron displacements to the aircraft aerodynamic forces.

C. Aileron Mass Uncertainty

The aileron structural model is shown in Fig. 7. Its inertial properties are defined by the lumped mass elements associated with the aileron structural grid points. The effects of the mass variations are considered in x (chordwise) and z (vertical) directions. Define the vector of the aileron masses in the directions of interest as

$$\boldsymbol{m}_{\text{ail}} = \begin{bmatrix} \boldsymbol{m}_T & \boldsymbol{m}_{M_u} & \boldsymbol{m}_{M_l} & \boldsymbol{m}_{L_u} & \boldsymbol{m}_{L_l} \end{bmatrix}^T \tag{46}$$

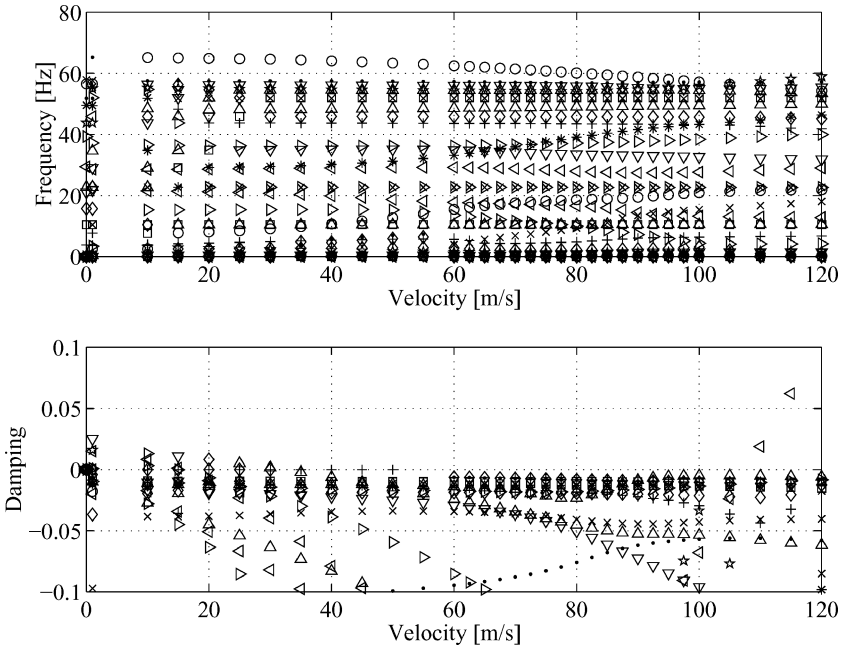

Fig. 6 Close-loop flutter analysis.

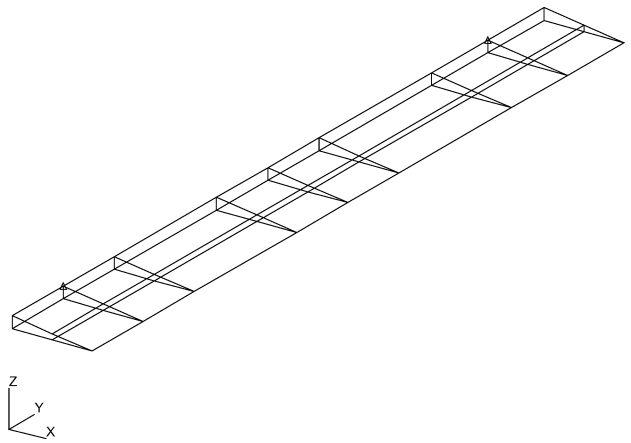

Fig. 7 Aileron structural model.

where $\boldsymbol{m}_T$, $\boldsymbol{m}_{M_u}$, $\boldsymbol{m}_{M_l}$, $\boldsymbol{m}_{L_u}$, and $\boldsymbol{m}_{L_l}$ are the $1 \times 2n_{\text{gr}}$ row vectors of the x and z masses in the grid points of the trailing-edge span, upper and lower middle spans, and upper and lower leading-edge spans; and $n_{\text{gr}} = 9$ is the number of grids in a span.

The mass matrix under consideration is $[M_{vv}] = \text{diag}(m_{\text{ail}})$, and the matrix of structural variations is expressed as

$$\bar{\Delta}_{\text{st}} = W_{\text{sm}}[M_{vv}]\Delta_m \tag{47}$$

where W_{sm} is the $n_v \times n_v$ scaling matrix, $n_v = 5 \cdot 2n_{\text{gr}} = 90$ is the number of degrees of freedom involved in the variation (where 5 is the number of the aileron spans), and the normalized uncertainty matrix Δ_m is expressed as

$$\Delta_m = \text{diag}\left(\delta_{m1} I_{2n_{\text{gr}}}, \delta_{m2} I_{2n_{\text{gr}}}, \delta_{m3} I_{2n_{\text{gr}}}, \delta_{m4} I_{2n_{\text{gr}}}, \delta_{m5} I_{2n_{\text{gr}}}\right) \tag{48}$$

where δ_{mi} are the real scalar values satisfying $|\delta_{mi}| \leq 1$ and $I_{2n_{\text{gr}}}$ is the $2n_{\text{gr}} \times 2n_{\text{gr}}$ unity matrix.

The uncertainties δ_{mi} correspond to the masses located in the five aileron spans: δ_{m1}, trailing-edge span; δ_{m2} and δ_{m3}, upper and lower middle spans; and δ_{m4} and δ_{m5}, upper and lower leading-edge spans. Therefore, the model addresses the uncertainty in the chordwise mass distribution of the aileron. The scaling matrix W_{sm} defines the maximal relative uncertainty of 10% of the nominal mass values: $W_{\text{sm}} = 0.1 I_{2n_v}$.

The modern multi-input/multi-output approach for robust stability analysis is based on the small gain theorem,[14] which addresses

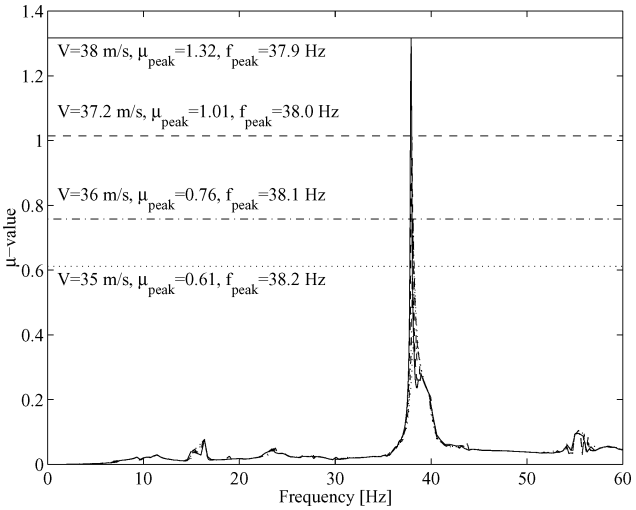

Fig. 8 Structured singular values of open-loop ASE system for mass uncertainty.

the stability of the P–Δ feedback system. For the ASE systems, a transfer matrix $P(i\omega)$ is defined by Eq. (22) and $\Delta(i\omega)$ is the normalized uncertainty feedback matrix of Eq. (20). To determine the robust stability of the system, the maximum value of the structured singular value $\mu_\Delta[P(i\omega)]$ over the entire frequency range $\omega \in [0, \infty]$ must be computed. If this value is less than unity, the system is stable for all $\Delta \in \boldsymbol{\Delta}$ and $\|\Delta\|_\infty < 1$, where $\boldsymbol{\Delta}$ is the set of possible structured uncertainties (defined by the block-diagonal structure of the matrix Δ_m in the case under consideration). The small gain theorem establishes stability of systems with uncertainties, whereas the nominal system $P(i\omega)$ is stable. As mentioned earlier, the test-case ASE system contains two rigid-body modes, and so it is not stable. To satisfy the conditions of the small gain theorem, the zero frequencies of the rigid-body modes are replaced by frequencies of 0.1 Hz with corresponding changes of the modal matrices. As a result, the frequency response alters in the vicinity of zero frequency only, which is not important for analysis of dynamic stability of the system.

The results of the open-loop robust stability analysis performed for several aircraft velocities are presented in Fig. 8. (The μ values were calculated by using the MATLAB® μ-Analysis and Synthesis Toolbox.[15]) The μ value reaches unity at the robust flutter velocity of

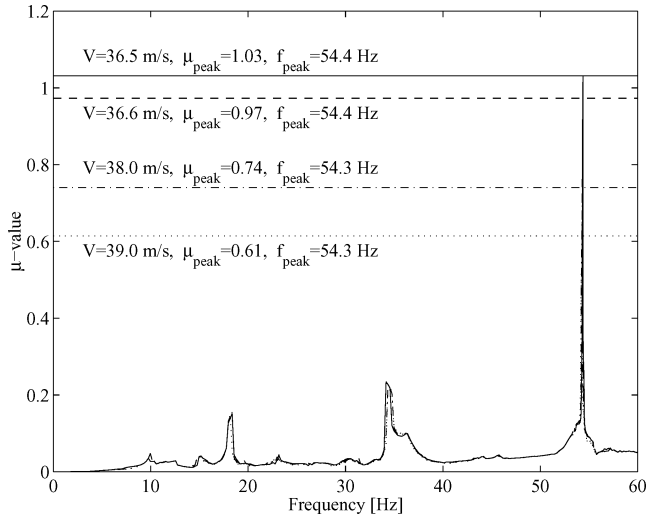

Fig. 9 Structured singular values of closed-loop ASE system for mass uncertainty and airspeed corresponding to first flutter mechanism.

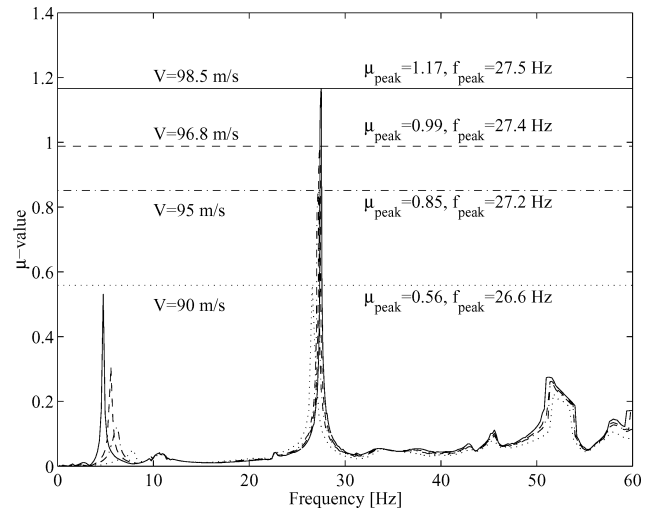

Fig. 10 Structured singular values of closed-loop ASE system for mass uncertainty and airspeed corresponding to second and third flutter mechanisms.

37.2 m/s with the frequency of 38.0 Hz, which is 8.4% lower than the nominal flutter velocity. The results of the closed-loop robust stability analysis shown in Figs. 9 and 10 demonstrate that the robust flutter velocities of the first and the third flutter mechanisms draw nearer to each other in comparison with the flutter velocities of the nominal system. Hence, the aileron mass uncertainty narrows the range of stability of the closed-loop ASE system. The low-frequency μ peak corresponding to the second flutter mechanism (Fig. 10) is considerably less than unity, and so this mechanism does not have an effect on robust stability of the system. It can be observed that the μ-value curve of the open-loop system (Fig. 8) has practically no peaks, except the one corresponding to the flutter frequency. This peak is suppressed by the control system and is not observed in the μ plots of the closed-loop ASE system. On the other hand, the μ curve obtained for the first flutter mechanism of the closed-loop system (Fig. 9) demonstrates two peaks (in the vicinity of 18 and 35 Hz) corresponding to the first wing torsion and to the third wing bending structural modes, both of which contain the aileron rotation.

D. Aileron Aerodynamic Uncertainty

The UAV aerodynamic model shown in Fig. 4 consists of 156 aerodynamic boxes and has $n_k = 312$ aerodynamic degrees of freedom, which are the heave and pitch motions defined for every box. The panel representing the aileron contains 18 aerodynamic boxes (3 chordwise boxes × 6 spanwise boxes) and has $n_{v_a} = 36$ aerodynamic degrees of freedom. Consider uncertainties in those elements of the $n_k \times n_k$ AIC matrix that relate the deflections in the aileron degrees of freedom to the aerodynamic forces of the entire aerodynamic model. In this case, the matrix $[\mathrm{AIC}_{kv_a}]$ of the perturbed AICs has n_k rows and n_{v_a} columns. Consider three spanwise strips of the aileron aerodynamic model and, following the approach of Borglund,[4] suppose that the AICs corresponding to deflections of the aerodynamic boxes of each strip deviate in a uniform manner.

The matrix of aerodynamic variation is expressed as

$$\bar{\Delta}_a = W_{sa}\left[\mathrm{AIC}_{kv_a}\right]\Delta_a \tag{49}$$

where $W_{sa} = \mathrm{diag}(0.1I_{2n_{\mathrm{sp}}}, 0.1I_{2n_{\mathrm{sp}}}, 0.1I_{2n_{\mathrm{sp}}})$ is the $n_{v_a} \times n_{v_a}$ scaling matrix defining the maximal relative uncertainties of 10% for all span strips, $\Delta_a = \mathrm{diag}(\delta_{l_1} I_{n_{\mathrm{sp}}}, \delta_{p_1} I_{n_{\mathrm{sp}}}, \delta_{l_2} I_{n_{\mathrm{sp}}}, \delta_{p_2} I_{n_{\mathrm{sp}}}, \delta_{l_3} I_{n_{\mathrm{sp}}}, \delta_{p_3} I_{n_{\mathrm{sp}}})$, $|\delta_{li}|, |\delta_{pi}| \leq 1$ are the complex scalars corresponding to uncertainties in the heave and pitch motions of the three spanwise strips of the aileron model, and $n_{\mathrm{sp}} = 6$ is the number of spanwise boxes.

As shown in Fig. 11, the open-loop robust flutter velocity is 34.7 m/s with the frequency of 37.9 Hz, which is 14.5% lower than the nominal flutter velocity. The closed-loop robust flutter velocity for the first flutter mechanism is 35.4 m/s, with the frequency of 54.5 Hz (Fig. 12). The aerodynamic uncertainty does not have

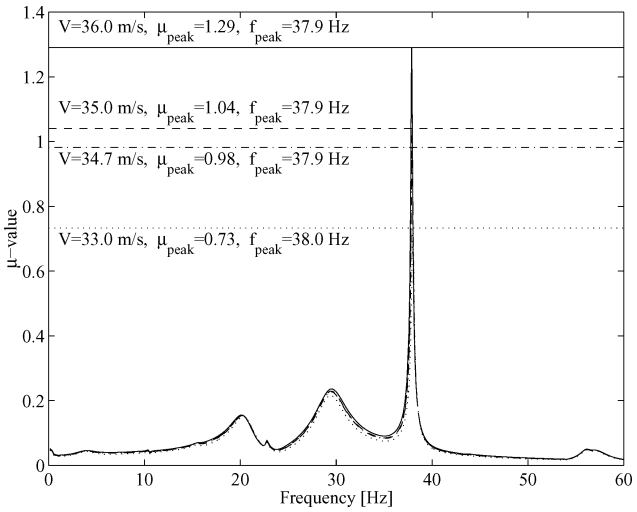

Fig. 11 Structured singular values of open-loop ASE system for aerodynamic uncertainty.

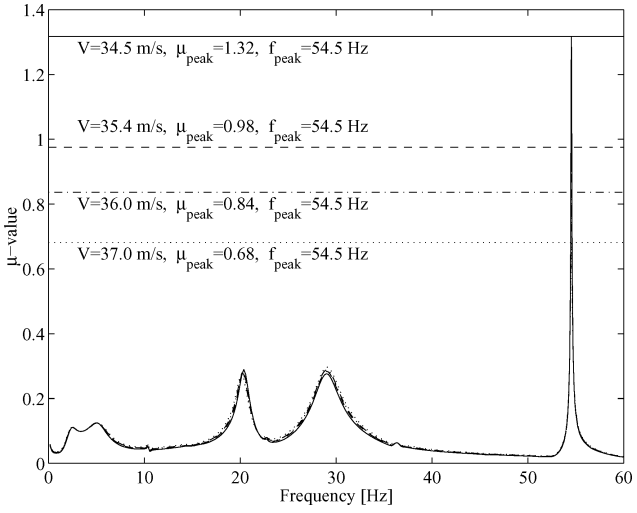

Fig. 12 Structured singular values of closed-loop ASE system for aerodynamic uncertainty and airspeed corresponding to first flutter mechanism.

Table 1 Stability ranges of ASE systems

System	Stability range, m/s		
	Open loop	Closed loop	Overlap
Nominal	0.0–40.6	32.2–100.3	32.2–40.6
Mass uncertainty	0.0–37.2	36.6–96.8	36.5–37.2
Aero uncertainty	0.0–34.7	35.4–81.0	——

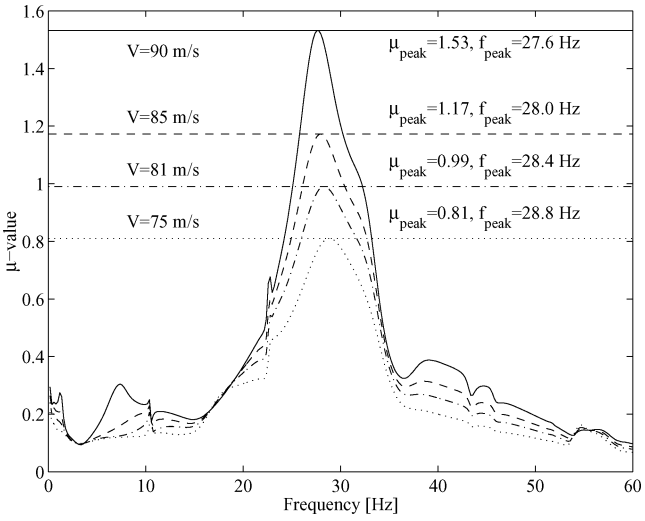

Fig. 13 Structured singular values of closed-loop ASE system for aerodynamic uncertainty and airspeed corresponding to second and third flutter mechanisms.

an effect on the flutter velocity for the second flutter mechanism (Fig. 13). On the other hand, the robust flutter velocity for the third flutter mechanism becomes 81.0 m/s with the frequency of 28.4 Hz, which is 19.2% lower than the nominal flutter velocity for this mechanism. The third flutter mechanism and the first wing torsion mode become apparent in the μ-value curves of Figs. 11 and 12 due to the peaks in the vicinities of 30 and 20 Hz.

Stability ranges for the nominal and uncertain ASE systems presented in Table 1 demonstrate that the mass uncertainty reduces the range of overlap stability of the open- and closed-loop systems to 0.7 m/s, whereas the aerodynamic uncertainty leads to the vanishing of this overlap range.

IX. Conclusions

The methodology for modeling of uncertain or perturbed ASE systems is developed in this study. It provides efficient tools for constructing LFT models of ASE systems with uncertain or variable structural and aerodynamic parameters. The general approach for modeling of structural and aerodynamic variations in frequency and time domains, as well as in discrete and modal coordinates, is presented. The use of structured uncertainties to represent perturbations and variations in the ASE model minimizes the uncertainty over-bounding. The models constructed using the developed technique allows one to perform open- and closed-loop robust stability and performance analyses, robust control synthesis, and multidisciplinary optimization of the uncertain or perturbed ASE systems. Application of this technique was demonstrated building models and performing robust stability analysis for a UAV with inertial and aerodynamic uncertainties in its control surface.

Acknowledgment

The work presented in this paper was supported by a joint grant from the Israeli Ministry of Immigrant Absorption and the Council for Higher Education.

References

[1]Lind, R., and Brenner, M., *Robust Aeroservoelastic Stability Analysis*, Springer Verlag, London, 1999, pp. 67–113.

[2]Lind, R., "Match-Point Solutions for Robust Flutter Analysis," *Journal of Aircraft*, Vol. 39, No. 1, 2002, pp. 91–99.

[3]Borglund, D., "Robust Aeroelastic Stability Analysis Considering Frequency-Domain Aerodynamic Uncertainty," *Journal of Aircraft*, Vol. 40, No. 1, 2003, pp. 189–193.

[4]Borglund, D., "The μ–k Method for Robust Flutter Solutions," *Journal of Aircraft*, Vol. 41, No. 5, 2004, pp. 1209–1216.

[5]Moulin, B., Idan, M., and Karpel, M., "Aeroservoelastic Structural and Control Optimization Using Robust Design Schemes," *Journal of Guidance, Control, and Dynamics*, Vol. 25, No. 1, 2002, pp. 152–159.

[6]Rodden, W. P., and Johnson, E. H., "MSC/NASTRAN Aeroelastic Analysis User's Guide," MacNeal Schwendler Corp., Los Angeles, 1994.

[7]ZAERO Ver. 7.0. Theoretical Manual, ZONA Technology, Inc., Scottsdale, AZ, Nov. 2003.

[8]Idan, M., Karpel, M., and Moulin, B., "Aeroservoelastic Interaction Between Aircraft Structural and Control Design Schemes," *Journal of Guidance, Control, and Dynamics*, Vol. 22, No. 4, 1999, pp. 513–519.

[9]Karpel, M., "Time-Domain Aeroservoelastic Modeling Using Weighted Unsteady Aerodynamic Forces," *Journal of Guidance, Control, and Dynamics*, Vol. 13, No. 1, 1990, pp. 30–37.

[10]Zole, A., and Karpel, M., "Continuous Gust Response and Sensitivity Derivatives Using State-Space Models," *Journal of Aircraft*, Vol. 31, No. 5, 1994, pp. 1212–1224.

[11]Moulin, B., Feldgun, V., and Karpel, M., "Application of the State-Space Equation of the Integrated System in Stability and Response Analyses Including Sensitivity Evaluation," Faculty of Aerospace Engineering, Technical Rept. TAE No. 899, Technion—Israel Inst. of Technology, Haifa, Israel, July 2002.

[12]Moulin, B., "Robust Controller Design for Active Flutter Suppression," AIAA Paper 2004-5115, Aug. 2004.

[13]Karpel, M., Moulin, B., and Chen, P. C., "Extension of the g-Method Flutter Solution to Aeroservoelastic Stability Analysis," *Journal of Aircraft*, Vol. 42, No. 3, 2005, pp. 789–792.

[14]Zhou, K., Doyle, J. C., and Glover, K., *Robust and Optimal Control*, Prentice–Hall, Upper Saddle River, NJ, 1996, pp. 271–300.

[15]Balas, G. J., Doyle, J. C., Glover, K., Packard, A., and Smith, R., "μ-Analysis and Synthesis Toolbox for Use with MATLAB. User's Guide. Version 3," MathWorks, Inc., Natick, MA, 1998.

E. Livne
Associate Editor